

Integration of digital maxillary dental casts with 3D facial images in orthodontic patients: A three-dimensional validation study

Zhuoxing Xiao^a; Zijin Liu^a; Yan Gu^b

ABSTRACT

Objective: To evaluate three-dimensional (3D) accuracy and reliability of nonradiographic dentofacial images integrated with a two-step method.

Methods: 3D facial images, cone-beam computed tomography (CBCT) images and digital maxillary dental casts were obtained from 20 pre-orthodontic subjects. Digital dental casts were integrated into 3D facial images using a two-step method based on the anterior tooth area. 3D coordinate values of five dental landmarks were identified in both dentofacial images and CBCT images. The accuracy of the integration method was assessed with paired *t*-tests between dentofacial images and CBCT-based reference standards. Intraclass correlation coefficients (ICCs) were assessed for the reliability of dentofacial images and CBCT-based images. Analysis of variance and Kruskal-Wallis tests evaluated the accuracy of the method in different dimensions.

Results: There was no statistical difference between dentofacial images and CBCT reference standards in both translational and rotational dimensions ($P > .05$). Translational mean absolute errors for full dentitions were within 0.42 mm and ICCs were over 0.998 in *x*, *y*, and *z* directions. Rotational mean absolute errors for full dentitions were within 0.92° and ICCs over 0.734 in pitch, yaw, and roll orientations. Integration errors were significantly greater in the first molar, *z*-translation, and pitch rotation ($P < .05$).

Conclusions: Integrating 3D dentofacial images with the two-step method is precise and acceptable for clinical diagnostics and scientific purposes. Errors were greater in the molar region, *z*-translation, and pitch rotation. (*Angle Orthod.* 2020;90:397–404.)

KEY WORDS: 3D dentofacial image; Integration; Validation study; Orthodontics

INTRODUCTION

Intraoral and facial photographs, dental casts, and a routine set of two-dimensional (2D) radiographs have been obtained for orthodontic diagnosis and treatment planning for decades.¹ Recent studies suggested that lateral cephalometric radiographs were dispensable for most orthodontics treatment decisions.² Noninvasive imaging systems including laser scanners,³ stereophotogrammetry,⁴ and structured light imaging systems⁵ were developed for facial measurement. Several studies have attempted to integrate digital dental models into three-dimensional (3D) facial images to simulate the anatomic dentofacial structure.^{6–8} Manosudprasit et al.⁹ evaluated the agreement between nonradiographic 3D dentofacial images and standard orthodontic records for orthodontic diagnosis and treatment planning. They found most diagnostic and treatment decisions reached fair agreement between the two records. Masoud et al.¹⁰ established male and

^a Postgraduate Student, Department of Orthodontics, National Engineering Laboratory for Digital and Material Technology of Stomatology, Beijing Key Laboratory of Digital Stomatology, Peking University School and Hospital of Stomatology, Beijing, China.

^b Professor, Department of Orthodontics, National Engineering Laboratory for Digital and Material Technology of Stomatology, Beijing Key Laboratory of Digital Stomatology, Peking University School and Hospital of Stomatology, Beijing, China.

Corresponding author: Dr Yan Gu, Department of Orthodontics, Peking University School and Hospital of Stomatology, No. 22 Zhongguancun Avenue South, Haidian District, Beijing, 100081, China
(e-mail: guyan96@126.com)

Accepted: November 2019. Submitted: July 2019.

Published Online: January 20, 2019

© 2020 by The EH Angle Education and Research Foundation, Inc.



Figure 1. 3D facial photographs, CBCT images and virtual dental cast acquisition. (A–C) 3D facial image acquisition. (D–E) CBCT image acquisition. (F) Digital maxillary dental cast in STL format with five landmarks.

female reference values of 3D dentofacial photogrammetry for orthodontic diagnosis. Castillo et al.¹¹ investigated the correlation between nonradiographic 3D photogrammetry measurements and corresponding traditional cephalometric measurements, suggesting that 3D photography was a significant predictor of the cephalometric measurements. Since some countries have already passed legislation to prohibit the use of radiographs after orthodontic treatment,¹² nonradiographic dentofacial photography might serve as a suitable substitution.

Previous validation studies were limited to anterior teeth or the first premolar.^{6,7} However, some vital anthropometric parameters of 3D dentofacial images, including molar position and cant of the occlusal plane, have not been validated.¹³ In addition, validation methods of previous studies were limited to root mean square (RMS)⁶ or 2D linear measurements.⁷ 3D validation studies of dentofacial photography are generally unavailable. The aim of the present study was to evaluate 3D accuracy and reliability of the nonradiographic dentofacial image compared with cone-beam computed tomography (CBCT) based standard references.

MATERIALS AND METHODS

This research was approved by the Institutional Review Board of Peking University School and Hospital of Stomatology (PKUSSIRB-201839148). Twenty healthy subjects (six males, 14 females; mean

age: 24.5 ± 9.3 years) ready for pre-orthodontic examinations in Peking University School and Hospital of Stomatology were enrolled in the study from January 2019 to March 2019. Inclusion criteria included: (1) required CBCT examinations, (2) complete permanent dentition, and (3) no history of orthodontic treatment. Subjects with crown restorations and history of maxillofacial trauma or maxillofacial surgery were excluded. A written informed consent was obtained from each participant.

Image Acquisition

3D facial photographs were acquired with the 3D optical FaceSCAN3D system (3D-Shape, Erlangen, Germany).⁵ Patients were instructed to sit in a natural head position with eyes closed. Two facial images were obtained: one at rest with teeth in occlusion (Figure 1A), and the other with exposure of anterior teeth using cheek retractors (Figure 1B).⁶ All 3D facial photographs were filmed by a postgraduate student (ZX.X) (Figure 1C).

CBCT scans (i-CAT System, Imaging Sciences International, Hatfield, PA, USA) were taken under the following conditions: 120 kV; 5 mA; voxel size, 0.3 mm; and exposure time 3,708 ms. Patients were asked to sit in the same posture as in the 3D facial filming process (Figure 1D). CBCT scans were processed in Materialise Mimics software (Materialise NV, Leuven, Belgium, version 17.0); skeletal and facial soft tissues

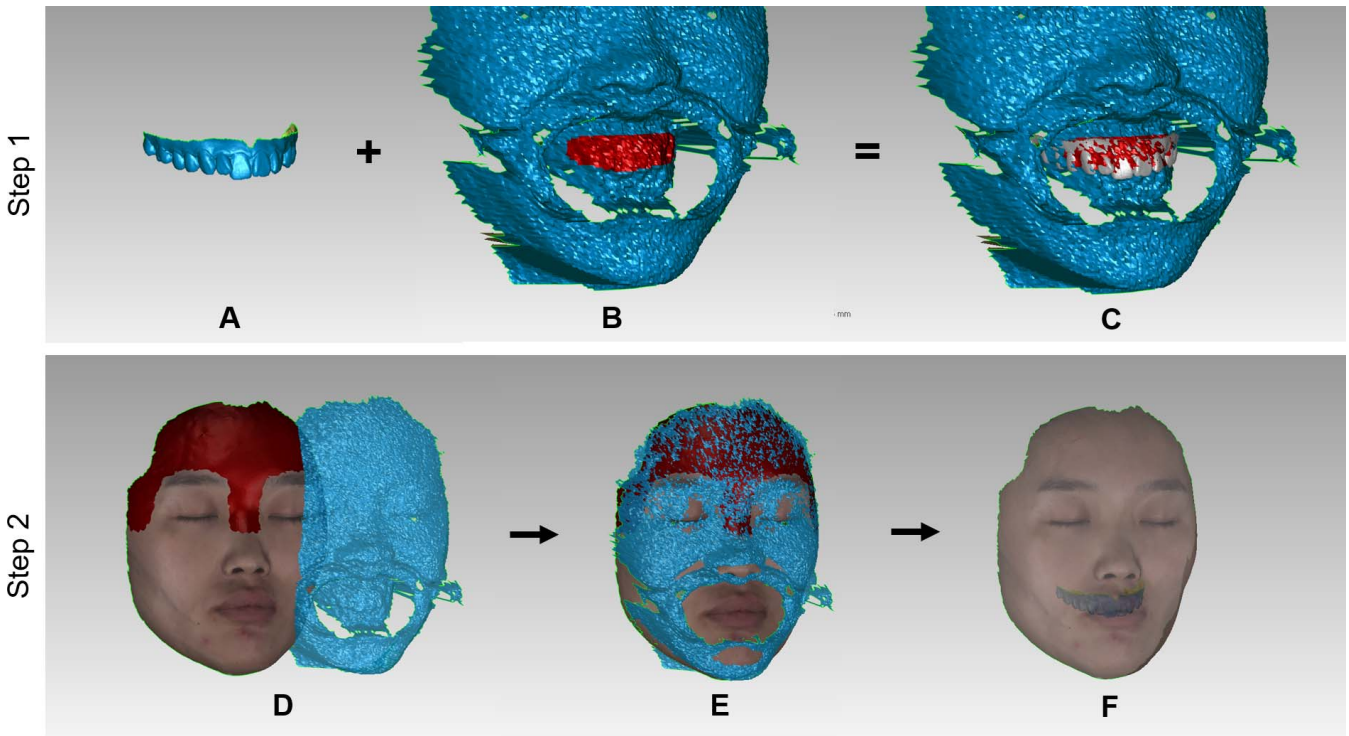


Figure 2. 3D facial image-based dentofacial model superimposition. (A–C) Step 1: registration of dental model into facial image (cheek retractor). (D–F) Step 2: registration of facial image (cheek retractor) with facial image (at rest). Red region indicates registration reference areas.

were segmented and exported as STL files (Figure 1E).

Plaster casts were digitized with a 3D laser scanner (R900, 3Shape, Copenhagen, Denmark). Each scan was exported as STL files and analyzed with Geomagic Studio software (ver. 2014; Geomagic International, Morrisville, NC, USA). Five landmarks (mesioincisal edge of tooth 11, cusp tip of teeth 13 and 23, mesiobuccal cusp of teeth 16 and 26) were assigned to each dental model according to a previous publication (Figure 1F).¹⁴

Construction of 3D Facial Image-Based Dentofacial Images

3D facial images and digital dental models were imported into Geomagic software. Two steps were necessary to integrate the dental model into the 3D facial image (Figure 2).⁷ Step 1: to improve registration accuracy, only the dental crown and attached gingiva region on the dental model were isolated. The registration reference area was selected on the facial image (cheek retractor). Because the canine is at the corner of the dental arch, posterior teeth were blocked partially during filming, where the image of the teeth became inaccurate for registration. Therefore, registration reference areas could be selected at least from

canine to canine in most cases. Then, global registration was performed. Step 2: the registration reference areas were selected on the 3D facial image (at rest), including the forehead, nasal root and zygoma regions.¹⁵ After global registration, the facial image (cheek retractor) was removed and a 3D dentofacial image was constructed (Figure 2F).

Construction of CBCT-Based Dentofacial Images as the Reference Standard

To eliminate the error of landmark identification, the identical digital dental model (with landmarks) was fused into the CBCT image (Figure 3, Step 3). The registration method and its accuracy were introduced in previous studies.^{16,17} The gingival area and interproximal contact region were removed from the digital dental model. After global registration, the skeletal portion was removed. The CBCT-based image was integrated into the 3D dentofacial image for unification into the same coordinate system (Figure 3, Step 4). The facial soft tissue surface was selected as the registration reference area on the 3D facial image, excluding the periorbital, nasolabial, and submandibular regions.¹⁵

Root mean square (RMS) between registration reference surfaces are presented in color-coded maps

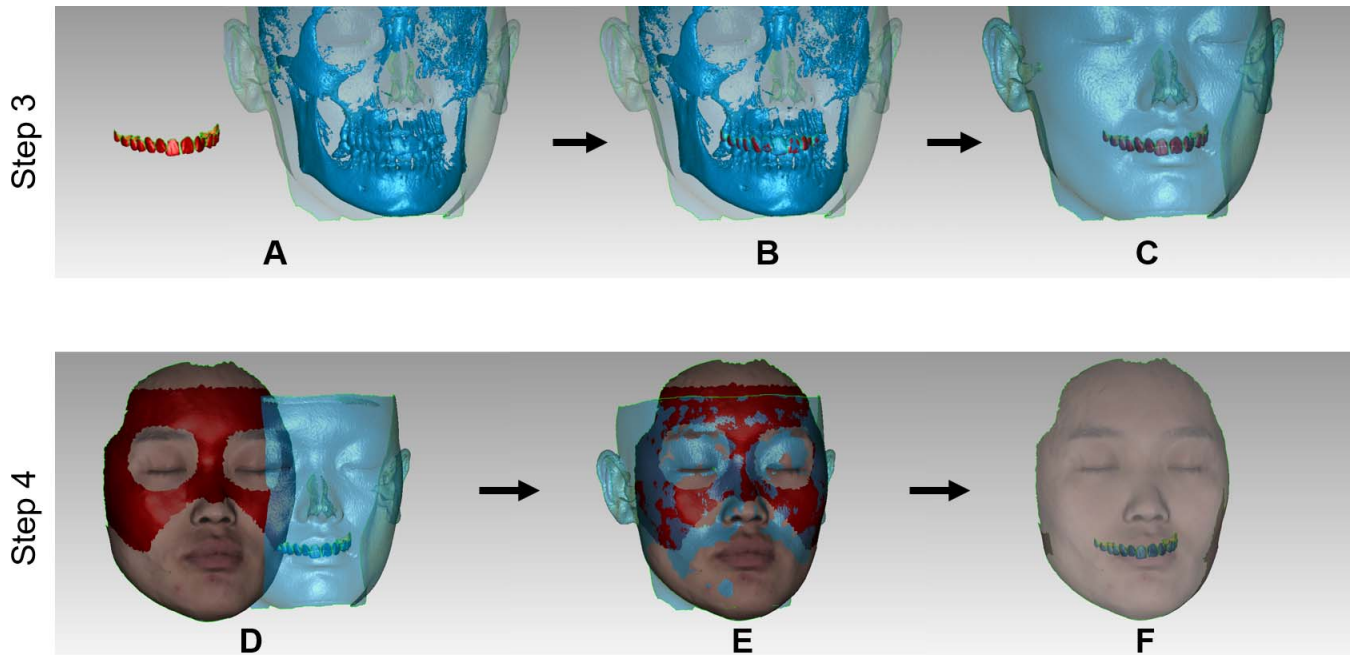


Figure 3. CBCT-based dentofacial image superimposition. (A–C) Step 3: registration of dental model into CBCT image. (C) CBCT-based dentofacial image. (D–F) Step 4: registration of two sets of dentofacial models. Red region indicates registration reference areas.

(Figure 4). The RMS value was calculated with the following equation:

$$\text{RMS} = \sqrt{\frac{1}{n}(x_1^2 + x_2^2 + \dots + x_n^2)}$$

Construction and Unification of 3D Coordinate System

A 3D coordinate system was generated with the midpoint of the bilateral trignon (T) as the origin (0,0,0), the line through bilateral trignon from right to left as the x-axis, and soft tissue Frankfort horizontal (FH) plane as the x-z plane (Figure 4E). Soft tissue FH plane was introduced in a previous study.¹⁸ In this coordinate system, positional differences between two sets of dentofacial models in six dimensions (Figure 4E), three translational directions (x, y, and z), and three rotational orientations (pitch, yaw, roll) were measured through 3D coordinate values of the five dental landmarks.

Two postgraduate students (ZX.X and ZJ.L) performed the registration procedures independently. The registration process was repeated in a two-week interval by ZX.X.

Statistical Analysis

Statistical tests were performed with SPSS 21.0 (IBM Corporation, Armonk, NY, USA). Intraclass correlation coefficients (ICCs) were used to evaluate

intra- and interoperator reliability of the dentofacial images and CBCT reference standards. Paired *t*-tests between the dentofacial images and CBCT-based reference standards were performed to evaluate the accuracy of the integration method. Analysis of variance and Kruskal-Wallis analysis were performed to assess the variance of method accuracy in different dimensions. Statistical significance were set at $P < .05$. Errors within 2 mm or 2° were considered as clinically acceptable.

RESULTS

Each registration step is shown separately in different color maps (Figure 4). Registration error of each step is presented in RMS values (Table 1). In four registration steps, mean RMS values between superimposition surfaces were <0.36 mm, which were in accordance with previous research.⁶ Mean RMS error between the integration method and reference standard was 0.37 mm.

ICCs of CBCT reference standards for intra- and interobserver reliabilities are shown in Table 2, which were close to 1.000. Absolute mean error between two repeated reference standards were within 0.07 mm in the five dental landmarks, indicating the CBCT reference standard to be precise and reliable.

The reliability and accuracy of the integration method are shown in Table 3. The results demonstrated a moderate to excellent method reliability, with ICC > 0.998 in translation, ICC (intra-observer) > 0.905 , and

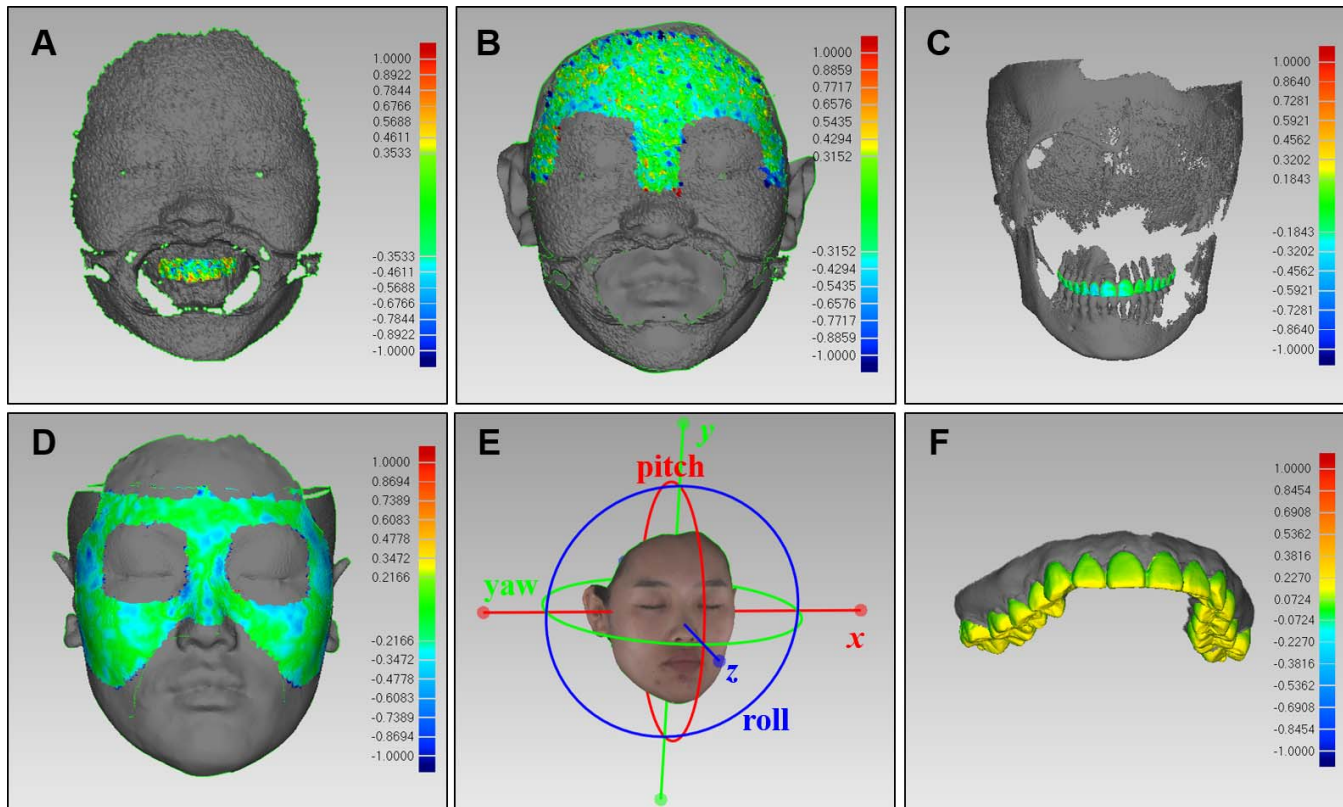


Figure 4. (A–D) Color-coded map of four registration steps. (A) Registration of digital dental model into 3D facial image (cheek retractor). (B) Registration of 3D facial image (at rest) into 3D facial image (cheek retractor). (C) Registration of laser-scanned dental model into CBCT image. (D) Registration of CBCT image into 3D facial scan (at rest). (E) 3D coordinate system with dental movement in six dimensions. (F) RMS between method and CBCT reference standard.

ICC (interobserver) > 0.734 in rotation. In the dimension of translation, no significant difference was observed between the method and reference standard ($P > .05$). For full dentition in translation, mean absolute deviations were within 0.42 mm in three directions, which was considered as clinically acceptable. Mean absolute total error between the integration method and the reference standard was 0.64 mm,

Table 1. Root Mean Square (RMS) Values Between Two Matched Surfaces After Registration Procedure^a

Registration Procedure	RMS Value (mm)
Registration of digital dental model into 3D facial image (cheek retractor)	0.36 ± 0.05 [0.28, 0.45]
Registration of 3D facial image (at rest) onto 3D facial image (cheek retractor)	0.30 ± 0.04 [0.23, 0.41]
Registration of laser-scanned dental model into CBCT image	0.21 ± 0.03 [0.17, 0.26]
Registration of CBCT image onto 3D facial image (at rest)	0.23 ± 0.06 [0.17, 0.38]
Difference between integration method and reference standard (CT0-T0)	0.37 ± 0.09 [0.19, 0.57]

^a RMS values are presented as mean ± standard deviation [range]. CT0, reference standard images constructed by observer 1 (ZX.X) at T0; T0, 3D dentofacial images constructed by observer 1 (ZX.X) at T0.

which was larger than that of the corresponding RMS value with statistical significance ($P < .05$). In the dimension of rotation, mean deviation of dentition rotation in pitch, yaw, and roll orientation were within 0.92 degree, which was clinically acceptable with no significant difference compared with the CBCT reference standard ($P > .05$).

The results of the variation analysis for accuracy of the method in different dimensions are shown in Figure 5. There was a significant difference between anterior and posterior teeth for mean absolute total errors of the method in translation ($P < .05$), with the molar group greater than that of the incisor group and the premolar group (Figure 5A). For translational errors of the full dentition in three directions, mean absolute errors in the x-direction were significantly greater than the other two directions ($P < .05$) (Figure 5B). For rotational errors in the full dentition, deviation in pitch orientation was significantly greater than that in yaw orientation ($P < .05$) (Figure 5C).

DISCUSSION

Since nonradiographic dentofacial images have a potential use as 3D records for orthodontic diagnosis

Table 2. Absolute Mean Error and ICCs of CBCT Reference Standard^a

	Abs Mean Error (mm) (CT0–CT1)	Intra-observer [95% CI] (CT0–CT1)	Interobserver [95% CI] (CT0–CT2)
I	0.07 ± 0.05 [0.00, 0.18]	1.000 [1.000, 1.000]	1.000 [1.000, 1.000]
PMR	0.07 ± 0.05 [0.00, 0.19]	1.000 [1.000, 1.000]	1.000 [1.000, 1.000]
PML	0.07 ± 0.05 [0.00, 0.19]	1.000 [1.000, 1.000]	1.000 [1.000, 1.000]
MR	0.07 ± 0.05 [0.00, 0.20]	1.000 [1.000, 1.000]	1.000 [1.000, 1.000]
ML	0.06 ± 0.04 [0.00, 0.19]	1.000 [1.000, 1.000]	1.000 [1.000, 1.000]

^a I indicates incisor group; PMR, right premolar group; PML, left premolar group; MR, right molar group; ML, left molar group. CT0 and CT1, reference standard images constructed by observer 1 (ZX.X) at T0 and T1; CT2, reference standard images constructed by observer 2 (ZJ.L).

and treatment planning, it is necessary to validate their accuracy and reliability in three dimensions. Rangel et al.⁶ used the average distance between matched surfaces to represent the accuracy of integration, for which they believed the accuracy of integration was 0.35 ± 0.32 mm. However, the reference surface they used was in the incisor region, which was approximately a flat plane. Therefore, that may only represent discrepancies in one dimension and may not detect errors from other dimensions. In the current study, RMS was compared with the corresponding Euclidean distance in a 3D coordinate system when measuring the dentofacial positional deviation between reference

standard and the tested method. The RMS values were significantly smaller than the actual three-dimensional distances calculated from coordinate values (Table 3, $P < .05$). Therefore, it suggested that RMS values may misestimate the accuracy of the integration method. Thus, five dental landmarks were chosen under the 3D coordinate system to evaluate authentic dentofacial positional deviations of the method in six dimensions (three translational and three rotational orientations).

Rosati et al.⁷ digitized three dental and three facial landmarks on virtual dentofacial reproductions and directly on the face. They evaluated the accuracy of the

Table 3. Accuracy and Reproducibility of the Integration Method in Translation and Rotation^a

Translation (mm)	Paired-sample <i>t</i> -test			ICC [95% CI]		
	Abs Mean Error (CT0–T0) (Mean ± SD)	Mean Error [95% CI]	<i>P</i>	Intra-observer (T0–T1)	Interobserver (T0–T2)	
I	Total	0.63 ± 0.22	–0.15 [–0.36, 0.05]	.137	1.000 [1.000, 1.000]	1.000 [1.000, 1.000]
	<i>x</i>	0.26 ± 0.17	0.04 [–0.11, 0.18]	.622	0.999 [0.997, 1.000]	0.998 [0.996, 0.999]
	<i>y</i>	0.22 ± 0.22	–0.00 [–0.15, 0.14]	.970	0.999 [0.998, 1.000]	1.000 [0.999, 1.000]
	<i>z</i>	0.44 ± 0.24	–0.17 [–0.40, 0.06]	.143	1.000 [1.000, 1.000]	1.000 [1.000, 1.000]
PMR	Total	0.68 ± 0.20	–0.22 [–0.46, 0.02]	.065	1.000 [1.000, 1.000]	1.000 [1.000, 1.000]
	<i>x</i>	0.25 ± 0.17	0.05 [–0.10, 0.19]	.487	0.999 [0.998, 1.000]	0.999 [0.998, 1.000]
	<i>y</i>	0.31 ± 0.22	0.08 [–0.10, 0.26]	.346	0.999 [0.997, 1.000]	0.999 [0.996, 0.999]
	<i>z</i>	0.44 ± 0.26	–0.20 [–0.43, 0.03]	.085	1.000 [1.000, 1.000]	1.000 [1.000, 1.000]
PML	Total	0.65 ± 0.21	–0.14 [–0.34, 0.07]	.179	1.000 [1.000, 1.000]	1.000 [1.000, 1.000]
	<i>x</i>	0.27 ± 0.17	0.05 [–0.09, 0.20]	.456	0.999 [0.999, 1.000]	0.999 [0.998, 1.000]
	<i>y</i>	0.33 ± 0.17	0.07 [–0.10, 0.25]	.398	0.999 [0.997, 1.000]	0.999 [0.998, 1.000]
	<i>z</i>	0.41 ± 0.26	–0.13 [–0.36, 0.09]	.232	1.000 [1.000, 1.000]	1.000 [1.000, 1.000]
MR	Total	0.86 ± 0.29	–0.28 [–0.58, 0.01]	.061	1.000 [0.999, 1.000]	1.000 [0.999, 1.000]
	<i>x</i>	0.27 ± 0.18	0.08 [–0.07, 0.23]	.274	0.999 [0.997, 1.000]	0.999 [0.997, 1.000]
	<i>y</i>	0.55 ± 0.39	0.19 [–0.12, 0.49]	.220	0.998 [0.995, 0.999]	0.998 [0.994, 0.999]
	<i>z</i>	0.43 ± 0.29	–0.19 [–0.42, 0.04]	.096	1.000 [1.000, 1.000]	1.000 [1.000, 1.000]
ML	Total	0.72 ± 0.24	–0.14 [–0.37, 0.09]	.226	1.000 [1.000, 1.000]	1.000 [1.000, 1.000]
	<i>x</i>	0.27 ± 0.18	0.09 [–0.06, 0.24]	.237	0.999 [0.998, 1.000]	0.999 [0.998, 1.000]
	<i>y</i>	0.43 ± 0.27	0.17 [–0.05, 0.40]	.126	0.998 [0.995, 0.999]	0.998 [0.994, 0.999]
	<i>z</i>	0.40 ± 0.25	–0.10 [–0.32, 0.12]	.340	1.000 [1.000, 1.000]	1.000 [1.000, 1.000]
FD	Total	0.64 ± 0.17	–0.19 [–0.42, 0.04]	.097	1.000 [1.000, 1.000]	1.000 [1.000, 1.000]
	<i>x</i>	0.26 ± 0.17	0.06 [–0.08, 0.21]	.383	0.999 [0.997, 0.999]	0.999 [0.997, 0.999]
	<i>y</i>	0.28 ± 0.19	0.10 [–0.05, 0.25]	.172	0.999 [0.998, 1.000]	0.999 [0.998, 1.000]
	<i>z</i>	0.42 ± 0.24	–0.16 [–0.38, 0.06]	.146	1.000 [1.000, 1.000]	1.000 [1.000, 1.000]
RMS vs total translation			0.27 [0.21, 0.32]	.001*		
Rotation (°)						
FD	Pitch	0.92 ± 0.70	0.35 [–0.10, 0.82]	.185	0.961 [0.905, 0.984]	0.920 [0.810, 0.968]
	Yaw	0.25 ± 0.23	–0.09 [–0.23, 0.05]	.235	0.905 [0.779, 0.961]	0.734 [0.441, 0.885]
	Roll	0.53 ± 0.41	–0.02 [–0.31, 0.31]	.915	0.928 [0.830, 0.971]	0.870 [0.702, 0.947]

* $P < .05$, according to paired-sample *t*-test between RMS and mean absolute total tooth deviation for accuracy evaluation.

^a FD indicates full dentition; CT0, reference standard images constructed by observer 1 (ZX.X) at T0; T0 and T1, 3D dentofacial images constructed by observer 1 (ZX.X) at T0 and T1. T2, 3D dentofacial images constructed by observer 2 (ZJ.L).

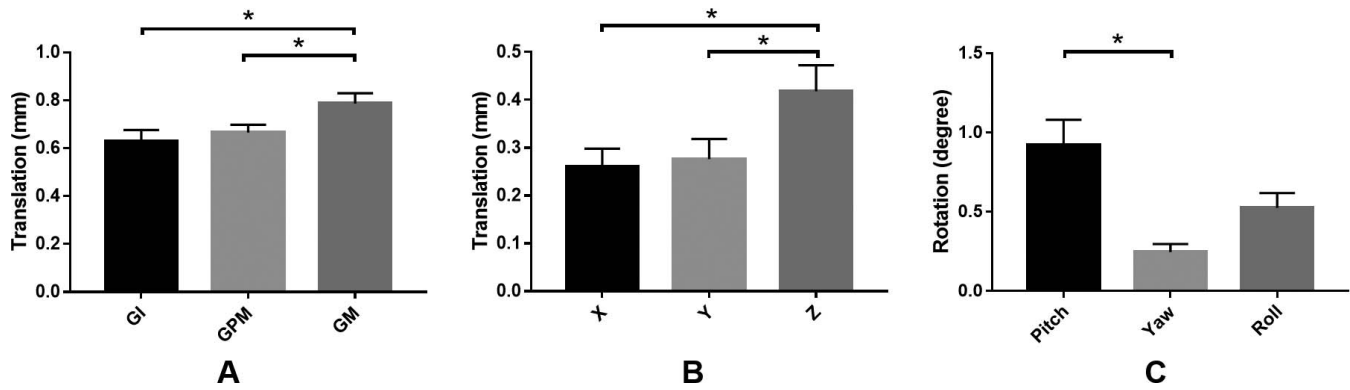


Figure 5. Difference of method accuracy in different dimensions. Values are presented as mean ± standard error; **P* < .05. (A) Difference of total mean absolute error in translation among incisor group (GI, 0.63 ± 0.22 mm), premolar group (GPM, 0.67 ± 0.21 mm), and molar group (GM, 0.79 ± 0.27 mm). (B) Difference of mean absolute dental displacement in translation among x (0.26 ± 0.17 mm), y (0.28 ± 0.19 mm), and z (0.42 ± 0.24 mm) orientations of full dentitions. (C) Difference for deviation in rotation of full dentition among pitch (0.92 ± 0.70 degree), yaw (0.25 ± 0.23°), and roll (0.53 ± 0.41°) orientations.

integration method by comparing seven linear measurements between virtual dentofacial reproduction and in direct measurement. Using manual anthropometric measurements as the reference standard, the majority of systematic errors probably were due to landmark identification. Relevant research concluded that the reproducibility of either measurement through manual anthropometry or that on 3D photography was unsatisfactory due to distortion of soft tissues and illegibility of anatomical structures.^{19,20} In this study, in order to reduce errors in landmark identification, a CBCT-based dentofacial image was chosen as reference standard.²¹ Five landmarks were digitized on the original digital dental model before the registration procedure. Subsequently, the original dental model was duplicated to the reference standard to avoid error from landmark identification. Previous studies illustrated the accuracy of registration between the CBCT and digital dental model,¹⁶ as well as that between the CBCT and 3D facial image.¹⁵ In this study, the mean absolute differences between repeated reference standard models were within 0.07 ± 0.05 mm and ICC values were close to 1.000 (Table 2), indicating that the CBCT-based reference standard was accurate and reliable.

Rangel et al.⁶ conducted measurements in the anterior tooth region. Rosati et al.⁷ extended measurement to the first premolars. With the lack of evaluation of the posterior part of the dentition, they were unable to measure the position of the molars and cant of the occlusal plane. In this study, measurements were extended to the first molars. For both the five dental landmarks and the full dentition, there were no significant differences between the reference standard and integration method (Table 3, *P* > .05). In addition, the accuracy of the integration method between anterior and posterior teeth was compared. Total mean

absolute error was significantly greater in the molar group compared with the incisor and premolar group (Figure 5A, *P* < .05). For the full dentition, translational error in the z-direction was significantly greater than the other two directions (Figure 5B, *P* < .05). However, the accuracy of the method was within 0.5 mm in all three directions, which was considered clinically acceptable (Table 3). Bechtold et al.¹⁴ integrated the dentofacial images in a 10-step method assisted with a transfer device. Using the same FaceSCAN3D system as in the current study, they reported greater integration errors in both the vertical and sagittal dimensions. Therefore, it was hypothesized that the two-step method in the present study could achieve higher precision without using an intricate transfer device. Additionally, rotational deviation in the pitch orientation was significantly greater than that in the yaw orientation (Figure 5C, *P* < .05). Nevertheless, rotational errors in all three orientations were marginal, with errors of tipping all < 1° (Table 3). In summary, the accuracy of the method in translational and rotational orientations was clinically acceptable.

The current study had several limitations. According to Rosati et al.⁷ and Bechtold et al.,¹⁴ they conducted similar studies with a sample size of 11 and 19, separately. In the current study, the sample size of 20 participants was acceptable; however, the predetermined sample size requirement was not achieved. In addition, although registrations were repeated by two operators, all facial scans were filmed by one operator (ZX.X). Adding operators for repeated filming would enhance the evaluation of the whole reproduction procedure in a more comprehensive manner. Additionally, the lower dentition was not evaluated in the current study. With the virtual occlusal record,²² the lower dentition could be transferred to the dentofacial

image, and adding this additional step should be tested in a future study.

CONCLUSIONS

- The 3D dentofacial image integrated with the two-step method used is precise and acceptable for clinical diagnostics and scientific purposes.
- The integration errors were greater in the molar region, in the z-orientation for translation, and in the pitch orientation for rotation.

ACKNOWLEDGMENTS

This work was supported by National Natural Science Foundation of China (NSFC 81771027, NSFC 81970979). We would like to thank Dr. Gui Chen, Yijiao Zhao, and Yong Wang, who offered their valuable advice on study design.

REFERENCES

1. Proffit WR, Fields H, Sarver D. *Contemporary Orthodontics*. 5th ed. St. Louis, MO: Mosby; 2012:169–211.
2. Durao AR, Alqerban A, Ferreira AP, Jacobs R. Influence of lateral cephalometric radiography in orthodontic diagnosis and treatment planning. *Angle Orthod*. 2015;85:206–210.
3. Gibelli D, Pucciarelli V, Poppa P, et al. Three-dimensional facial anatomy evaluation: reliability of laser scanner consecutive scans procedure in comparison with stereophotogrammetry. *J Craniomaxillofac Surg*. 2018;46:1807–1813.
4. Weinberg SM. 3D stereophotogrammetry versus traditional craniofacial anthropometry: comparing measurements from the 3D facial norms database to Farkas's North American norms. *Am J Orthod Dentofacial Orthop*. 2019;155:693–701.
5. Modabber A, Peters F, Kniha K, et al. Evaluation of the accuracy of a mobile and a stationary system for three-dimensional facial scanning. *J CranioMaxillofac Surg*. 2016;44:1719–1724.
6. Rangel FA, Maal TJJ, Bergé SJ, et al. Integration of digital dental casts in 3-dimensional facial photographs. *Am J Orthod Dentofacial Orthop*. 2008;134:820–826.
7. Rosati R, De Menezes M, Rossetti A, Sforza C, Ferrario VF. Digital dental cast placement in 3-dimensional, full-face reconstruction: A technical evaluation. *Am J Orthod Dentofacial Orthop*. 2010;138:84–88.
8. Rangel FA, Chiu Y, Maal TJJ, Bronkhorst EM, Bergé SJ, Kuijpers-Jagtman AM. Does powdering of the dentition increase the accuracy of fusing 3D stereophotographs and digital dental casts? *Eur J Orthod*. 2016;38:440–445.
9. Manosudprasit A, Haghi A, Allareddy V, Masoud MI. Diagnosis and treatment planning of orthodontic patients with 3-dimensional dentofacial records. *Am J Orthod Dentofacial Orthop*. 2017;151:1083–1091.
10. Masoud MI, Bansal N, C. Castillo J, et al. 3D dentofacial photogrammetry reference values: a novel approach to orthodontic diagnosis. *Eur J Orthod*. 2017;39:215–225.
11. Castillo JC, Gianneschi G, Azer D, et al. The relationship between 3D dentofacial photogrammetry measurements and traditional cephalometric measurements. *Angle Orthod*. 2019;89:275–283.
12. Turpin DL. British Orthodontic Society revises guidelines for clinical radiography. *Am J Orthod Dentofacial Orthop*. 2008;134:597–598.
13. Celar A, Tafaj E, Graf A, Lettner S. Association of anterior and posterior occlusal planes with different Angle and skeletal classes in permanent dentitions. *J Orofac Orthop*. 2018;79:267–276.
14. Bechtold TE, Goz TG, Schaupp E, et al. Integration of a maxillary model into facial surface stereophotogrammetry. *J Orofac Orthop*. 2012;73:126–137.
15. Jayaratne YS, McGrath CP, Zwahlen RA. How accurate are the fusion of cone-beam CT and 3-D stereophotographic images? *PLoS One*. 2012;7:e49585.
16. Sun L, Hwang H, Lee K. Registration area and accuracy when integrating laser-scanned and maxillofacial cone-beam computed tomography images. *Am J Orthod Dentofacial Orthop*. 2018;153:355–361.
17. Ye N, Long H, Xue J, Wang S, Yang X, Lai W. Integration accuracy of laser-scanned dental models into maxillofacial cone beam computed tomography images of different voxel sizes with different segmentation threshold settings. *Oral Surg Oral Med Oral Pathol Oral Radiol*. 2014;117:780–786.
18. Chortrakarnkij P, Lonc D, Lin H, Lo L. Establishment of a reliable horizontal reference plane for 3-dimensional facial soft tissue evaluation before and after orthognathic surgery. *Ann Plast Surg*. 2017;78:S139–S147.
19. Düppe K, Becker M, Schönmeier B. Evaluation of facial anthropometry using three-dimensional photogrammetry and direct measuring techniques. *J Craniofac Surg*. 2018;29:1245–1251.
20. Fagertun J, Harder S, Rosengren A, et al. 3D facial landmarks: Inter-operator variability of manual annotation. *BMC Medical Imaging*. 2014;14:35.
21. Park J, Baumrind S, Curry S, Carlson SK, Boyd RL, Oh H. Reliability of 3D dental and skeletal landmarks on CBCT images. *Angle Orthod*. 2019;89:758–767.
22. Botsford KP, Frazier MC, Ghoneima AAM, Utreja A, Bhamidipalli SS, Stewart KT. Precision of the virtual occlusal record. *Angle Orthod*. 2019;89:751–757.